AIAA JOURNAL
Vol. 44, No. 5, May 2006

Mass Flow Boundary Conditions for Subsonic Inflow and Outflow Boundary

Adam Jirásek*
Swedish Defence Research Agency, SE-164 90 Stockholm, Sweden

The development and verification of an inflow and outflow mass flow boundary condition are described. In addition, an outflow Mach number boundary condition was implemented and tested. The main motivation behind the development of a mass flow boundary condition is a need to bridge the gap between the requirement of direct setting of mass flow as one of the most important parameters, and the difficulty of indirect control of mass flow using static pressure outflow and total states inflow boundary conditions. The mass flow and Mach number boundary conditions were verified in low-speed flow through a two-dimensional channel with constant area and in high-speed flow through the Royal Airforce Establishment M2129 S-duct with large separation. Special attention was paid to the behavior of the mass flow boundary conditions in choked flow.

Nomenclature

c = speed of sound
M = Mach number
$\dot{M}$ = total mass flow through boundary
$\dot{m}$ = local mass flow
p = pressure
R = universal gas constant
Re = Reynolds number
S = area
S_h = constant in Sutherland's law for dynamic viscosity
T = temperature
$\boldsymbol{w}$ = velocity vector (u, v)
γ = Poisson constant
λ = Laval number
μ = dynamic viscosity
ρ = density

Subscripts

av = average value
i = local value in ith mesh point
n = updated values of velocity and static and total pressure
r = required value of mass flow or Mach number
ref = reference values
0 = total values

Superscripts

k = kth iteration
$*$ = critical values

I. Introduction

THE mass flow and Mach number are parameters of special interest in internal aerodynamics. Rather than absolute values of static pressure and values of the total state, mass flow and Mach number, or their combinations, are parameters known before the numerical experiment, either as values specified by the customer or as data supplied from a wind-tunnel experiment. Other aerodynamic characteristics are required as their functions. The most common way of formulating boundary conditions for internal aerodynamics is to prescribe the total pressure p_0, total temperature T_0, and total density ρ_0 at the inflow and static pressure p at the outflow. The mass flow, Reynolds number, and Mach number are set indirectly in this way of formulating boundary conditions. Total pressure p_0, which is prescribed at the inflow is, however, subject to energetic loss in the flow and is not known at an outflow. It is, therefore, difficult to estimate the appropriate value of static pressure at an outflow and total pressure at an inflow to match mass flow, Mach number, or Reynolds number unless some kind of estimate of total pressure loss is known. Even so, the process may include several steps of iterations during which the correct values of the total states and static pressure at boundaries are finally found. If a number of configurations at several flow conditions is supposed to be put to test, the amount of work spent on tuning the appropriate values of total and static pressure at the boundaries might exceed an acceptable level. The problem becomes even more complicated when the mass flow through device is prescribed as a function of time[1] or when flow through a device is nonsteady due to elastic behavior of the construction.[2,3] In this case, any estimate of pressure time dependency would be almost impossible. The use of boundary conditions with mass flow as a parameter is not restricted to the field of internal aerodynamics only. In the analysis of the external flowfield around a body including the effect of the propulsion unit, the mass flow represents an excellent choice for defining the boundary conditions, hence avoiding the need to solve the extremely complicated flow through an engine.[4–9] This uniqueness is further strengthened by another feature of mass flow. As long as the construction of the engine inlet keeps the mass flow constant (no boundary-layer bleed, etc.), the boundary of the computational domain may be moved freely along the inlet path, thus, giving the engineers a great deal of freedom during analysis.

Slater[10] outlined a mass flow outflow boundary condition in which the value of static pressure at the outflow is relaxed to its appropriate value with respect to the time-marching iterations using a relaxation parameter. In addition, the outflow Mach number boundary condition was shown as well. Pelant and Adámek[11] formulated a system of boundary conditions for their computational fluid dynamics (CFD) solver. One of these boundary conditions deals with a mass flow boundary condition at outflow that is transformed to a rather complicated boundary condition prescribing velocity. Unfortunately, the distribution of mass flow at the boundary must be known.

The new set of mass flow boundary conditions that are developed here are valid for both inflow and outflow of the computational domain. An outflow Mach number boundary condition defined by a small modification to the outflow mass flow boundary condition was implemented as well. The mass flow is used in a similar fashion

Received 28 January 2005; presented as Paper 2005-4963 at the AIAA 23rd Applied Aerodynamics Conference, Toronto, ON, Canada, 6–9 June 2005; revision received 20 October 2005; accepted for publication 23 October 2005.

*Research Engineer, Division of Systems Technology; adam.jirasek@foi.se. Member AIAA.

as in Ref. 10 to set up an appropriate value of total or static pressure prescribed at the boundary. The pressure is, however, not relaxed in time but rather set exactly to the value required by a given value of mass flow or Mach number. Moreover, the new boundary conditions take into account local variations of mass flow or Mach number directly from the solution, so that no estimate of their distribution is needed. In addition, the novel mass flow boundary conditions were extensively tested in choked flow.

II. Basic Relations

A. Isentropic Flow Relations for One-Dimensional Flow

Provided the flow of air is isentropic, it is possible to derive relationships between the total states and static state values of density, pressure, and temperature[12]:

$$\rho = \rho_0\{1 + [(\gamma - 1)/2]M^2\}^{-1/(\gamma - 1)} \tag{1}$$

$$p = p_0\{1 + [(\gamma - 1)/2]M^2\}^{-\gamma/(\gamma - 1)} \tag{2}$$

$$T = T_0\{1 + [(\gamma - 1)/2]M^2\}^{-1} \tag{3}$$

The parameter $M = w/c$ is the local Mach number, which is a function of the local speed of the flow and the static speed of sound. The static speed of sound is defined as

$$c = \sqrt{\gamma RT} \tag{4}$$

Thus, Mach number is a parameter dependent on the local speed of flow and values of static density, static pressure, or static temperature. It is useful to tie the static and total state values via a parameter that is dependent on local velocity and total state values. This is done using a variable defined in a similar fashion as the Mach number, as the ratio of local speed of flow to the local critical speed of sound. The variable is λ, and it is defined as

$$\lambda = w/c^* \tag{5}$$

where $c^* = \sqrt{(\gamma RT^*)}$ is the critical speed of sound and T^* is the value of the static temperature at critical flow conditions. When an equation that builds a relation between the total speed of sound, the static speed of sound, and the speed of flow is used, namely,

$$c_0^2 = c^2 + [(\gamma - 1)/2]w^2 \tag{6}$$

it is easy to derive the equation for the critical speed of sound as a function of the total states only:

$$c^* = c_0\sqrt{2/(\gamma + 1)} \tag{7}$$

Thus, the Laval number λ becomes a function of local velocity and total states. It is then possible to construct the equations relating static and total states analogical to Eqs. (1–3) using Laval number λ instead of Mach number M, as follows:

$$\rho = \rho_0\{1 - [(\gamma - 1)/(\gamma + 1)]\lambda^2\}^{1/(\gamma - 1)} = \rho_0\left\{1 - [(\gamma - 1)/2]\left(w^2/c_0^2\right)\right\}^{1/(\gamma - 1)} \tag{8}$$

$$p = p_0\{1 - [(\gamma - 1)/(\gamma + 1)]\lambda^2\}^{\gamma/(\gamma - 1)} = p_0\left\{1 - [(\gamma - 1)/2]\left(w^2/c_0^2\right)\right\}^{\gamma/(\gamma - 1)} \tag{9}$$

$$T = T_0\{1 - [(\gamma - 1)/(\gamma + 1)]\lambda^2\} = T_0\left\{1 - [(\gamma - 1)/2]\left(w^2/c_0^2\right)\right\} \tag{10}$$

Finally, the relation between Mach number and Laval number is

$$M^2 = \frac{2\lambda^2}{(\gamma + 1) - (\gamma - 1)\lambda^2} \tag{11}$$

$$\lambda^2 = \frac{(\gamma + 1)M^2}{(\gamma - 1)M^2 + 2} \tag{12}$$

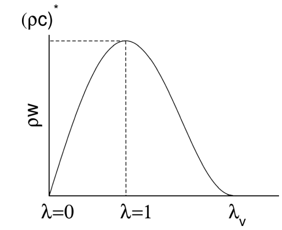

Fig. 1 Mass flow function.

B. Mass Flow

Mass flow through area S is defined as $\dot{m} = \rho w S$ and is shown as a function of Laval number λ in Fig. 1. The function has one maximum $\dot{m}^*$ defined by the condition $\partial\dot{m}/\partial\lambda = 0$ that occurs at $\lambda = 1$. At this speed, the flow is said to be choked, the mass flow is called critical mass flow, and its value is

$$\dot{m}^*/S = (\rho c)^* = \rho_0 c_0\sqrt{2/(\gamma + 1)}[1 - (\gamma - 1)/(\gamma + 1)]^{1/(\gamma - 1)} \tag{13}$$

It is the largest mass flow through unit area for given total states. The only way to change the value of critical mass flow is to change the values of total states. The mass flow is zero at $\lambda = 0$ and at the speed of flow into a vacuum $[\lambda_v = \sqrt{(\gamma + 1)/(\gamma - 1)}]$.

III. Formulation of New Boundary Conditions

Three boundary conditions are formulated: a mass flow boundary condition for an outflow boundary, a mass flow boundary condition for an inflow boundary, and a Mach number boundary condition for an outflow boundary.

At a subsonic outflow boundary, one boundary condition specified by user and four boundary conditions specified by interior flow are prescribed for three-dimensional flow. Generally, the boundary condition specified by the user is represented by specification of a value of static pressure. Unlike in the typical static pressure boundary conditions, in which the value of static pressure is given, the static pressure in the mass flow and Mach number outflow boundary condition is a function of the mass flow or Mach number, so that during the computational process the final value of the mass flow through the boundary or Mach number at the boundary reaches the desired value. Four conditions specified by interior flow are represented by extrapolation of density and the velocity vector. If part of the outflow boundary becomes supersonic, then all values of primitive variables at the supersonic part of the boundary are extrapolated, and no user-specified boundary condition is prescribed.

For the subsonic inflow boundary condition, four boundary conditions specified by the user and one boundary condition specified by the interior flow are required. The four conditions specified by the user are represented by specified values of the total pressure p_0, the total temperature T_0, and the direction of velocity vector (two directional angles). As in the case of the outflow mass flow and Mach number boundary conditions, the value of total pressure p_0 at the boundary is not fixed but is expressed as a function of mass flow so that during the iterational process the value of mass flow through the inflow boundary reaches the desired value. The boundary condition specified by interior flow is represented by an extrapolation of the Mach number from the interior of the computational domain.

A. Boundary Conditions with Prescribed Total Mass Flow

In the formulation of both inflow and outflow mass flow boundary conditions, the velocity vector is split into its component parts u normal to boundary and part v tangential to boundary so that $\boldsymbol{w} = (u, v)$.

1. *Outflow Mass Flow Boundary Condition*

At the outflow, the values of static pressure p, temperature T, and density ρ and velocity vector $\boldsymbol{w}$ are known from the solution at each time step of the iterational process. First, the total states p_0, ρ_0, and T_0 are calculated at each time step of the iterational process from the values of p, ρ, T, and w using Eqs. (1–3) or Eqs. (8–10) with Eq. (6). Now, provided that the mass flow $\dot{m}_r$ through the boundary is known, a new value of the velocity u_n normal to the boundary can be calculated. This value is obtained as the solution of an implicit equation for mass flow

$$\dot{m}_r = \rho_0 u_n \left\{1 - \left[(\gamma - 1)\big/2c_0^2\right]u_n^2\right\}^{1/(\gamma-1)} S \qquad (14)$$

where ρ_0 is known at each time step and $\dot{m}_r$ is the required value of mass flow. The new value of normal velocity u_n is then used to calculate a new value of Laval number λ_n

$$\lambda_n = u_n \big/ c^* \qquad (15)$$

Finally, a new value of static pressure p_n is then found as a function of the known value of total pressure p_0 and the value of λ_n [Eq. (9)]. The result is a new value of static pressure at the outflow boundary that corresponds to the required value of mass flow. If the static pressure boundary condition requires a uniform value of static pressure, the weighted average of all static pressures along the boundary

$$p_{\mathrm{av}_n} = \frac{\sum (p_n S)_i}{\sum S_i} \qquad (16)$$

is taken.

2. *Inflow Mass Flow Boundary Condition*

In this boundary condition, the mass flow is prescribed at the inflow. This boundary condition is completed by the value of total temperature T_0 and flow direction. The values of static pressure p, temperature T, and density ρ and velocity $\boldsymbol{w}$ at the boundary are known from the solution at each time step of the iterational process. The first step is to determine the new value of a normal component of velocity u_n. Because this boundary condition changes the total states at the inlet, it is not necessary to use Eq. (14) to calculate the normal component of velocity u. Instead, it can be calculated from the known value of mass flow $\dot{m}_r$ at each particular point at the boundary as

$$u_n = \dot{m}_r / \rho S \qquad (17)$$

The Laval number at each boundary point is then defined as

$$\lambda_n = w_n \big/ c^* = \sqrt{\left(u_n^2 + v_n^2\right)} \big/ c^* \qquad (18)$$

where the critical speed of sound c^* is a function of total temperature T_0 that is given, and where v_n is the tangential component of velocity that may be specified from the flow direction. When this value of the Laval number λ_n is used, a new total pressure p_{0_n} is calculated from the local static pressure p known from the solution using Eq. (9). If the total states boundary condition requires a uniform value of total pressure along the boundary, the weighted average value of all total pressures along the boundary is taken, analogous to Eq. (16).

3. *Determining the Distribution of Mass Flow at a Boundary*

As the input parameter to the inflow and outflow mass flow boundary condition, the total mass flow $\dot{M}_r$ through the entire boundary is given. However, the required distribution along the boundary may not be known. If this is the case, the following procedure is used to distribute the value of total mass flow along the boundary using the solution at a given time step. In each ith point on the boundary, the local mass flow is determined as $(\rho u)_i S_i$. The total mass flow through the boundary is then

$$\dot{M}_{\mathrm{tot}} = \sum_i [(\rho u)_i S_i]$$

The value of mass flow at each point on the boundary is then scaled to get the desired total mass flow $\dot{M}_r$ so that the local mass flow in the ith point is

$$\dot{m}_{i_r} = (\rho u)_i S_i (\dot{M}_r / \dot{M}_{\mathrm{tot}}) \qquad (19)$$

which is then the value used in Eqs. (14) and (17).

If the local value of mass flow given by Eq. (19) exceeds the value of local critical mass flow, as may happen at an outflow boundary, its value is limited so that no physical relations are violated. The value of total mass flow is then lower than the value required by the boundary condition. This lower value exists because the flow is choked somewhere upstream of the boundary, and, hence, the value of total mass flow is determined by the critical throat. This never happens at an inflow boundary because the total states are modified. If flow becomes choked downstream the inflow boundary the total states are modified so that the total value of mass flow through the boundary is equal to the critical mass flow.

B. Boundary Conditions with Prescribed Mach Number at the Outflow

As in the earlier case of mass flow boundary conditions, the value of the required Mach number is taken as an input parameter. The construction of the outflow Mach number has been made according to the formulation given in Ref. 10. It is simply reformulated so that its similarity with the mass flow boundary condition is apparent.

1. *Outflow Mach Number Boundary Condition*

At the outflow, the values of static pressure p, density ρ, and temperature T and velocity vector $\boldsymbol{w}$ are known from the solution at each time step of the iterational process. First, the total states are calculated from the static values of pressure, density, and velocity, viz., Sec. III.A.1.

Now, provided that the required local Mach number M_r at a particular point is known, the value of local Laval number λ_n may be found from Eq. (12). As in the case of the mass flow boundary condition, this value of local Laval number λ_n defines the new value of local static pressure p_n from the known value of total pressure p_0 and from using Eq. (9). As a result of the analysis, the new field of static pressure corresponding to the specific distribution of mass flow is obtained. If a uniform value of static pressure p is required, the average value of static pressure along the boundary is used.

2. *Determining the Distribution of Mach Number at the Boundary*

Unlike a mass flow, the definition of required Mach number M_r at a boundary is dependent on the definition given by the user. It is, hence, up, to the user to change the definition of the required Mach number and to update the calculation of the field of local Mach numbers accordingly. The example given here is for a required Mach number M_r defined as an averaged value of Mach numbers from all boundary points. First, the averaged Mach number

$$M_{\mathrm{av}} = \frac{\sum_i (w_i / c_i) S_i}{\sum_i S_i} \qquad (20)$$

is calculated. The value of reference Mach number M_r is then used to find a field of required local Mach numbers on the boundary point as

$$M_{i_r} = (w_i / c_i)(M_r / M_{\mathrm{av}}) \qquad (21)$$

C. Reynolds Number

If the Reynolds number Re is specified together with the Mach number or mass flow, a simple way of coupling these parameters may be derived. From the definition of unit Reynolds number $Re = \rho w / \mu$, the viscosity μ is determined by

$$\mu = \rho w / Re \qquad (22)$$

Then, the necessary step is to change the reference values in the law of dynamic viscosity μ. In Sutherland's law, the value of reference dynamic viscosity is given by

$$\mu_{\mathrm{ref}} = \mu (T_{\mathrm{ref}} / T)^{\frac{3}{2}} [(T + S_h)/(T_{\mathrm{ref}} + S_h)] \qquad (23)$$

where T_{ref} is given as an input parameter. The method of computing the value of the static temperature T used in Eq. (23) is strongly coupled with the way ρw is sampled and is dependent on user definition.

Procedures described in Secs. III.A.1, III.A.2, and III.B.1 are repeated at every time step of the iterational process. The values of static pressure p, static density ρ, static temperature T, and velocity $\boldsymbol{w}$, which are used in Eq. (17) and are needed to calculate the total states used in Eq. (14) are taken from the solution at the boundaries at every time step. Thus, the required values of static pressure p_n and total pressure p_{0_n} are updated regularly during the iterational process.

IV. Flow Solver

The CFD flow solver used for this study is Edge,[13] a finite volume Navier–Stokes solver for unstructured meshes. It employs local time stepping, local low-speed preconditioning, multigrid, and dual time stepping for steady-state and time-dependent problems. The data structure of the code is edge-based so that the code is constructed as a cell vertex. It can be run in parallel on a number of processors to solve large flow cases efficiently. It is equipped with a number of turbulence models based both on the eddy viscosity and an explicit algebraic Reynolds stress model (EARSM) assumption. The model that was used during this study was the two-equation k–ω model combined with Wallin and Johansson's EARSM[14] with compressible corrections.

The boundary conditions in the code are implemented in the weak formulation. The static pressure at the outflow and total states at the inflow boundary are used to calculate the numerical fluxes through the outflow or inflow boundary, respectively. The flow variables on the boundary are then updated using the same numerical scheme as the variables in the interior of the computational domain. The novel boundary conditions provide the original total states and static pressure boundary conditions with the appropriate values of the pressure; therefore, the numerical accuracy of the numerical scheme remains unchanged.

Because the code is a cell-vertex code with flow variables stored in the mesh nodes, the values of flow variables needed in boundary condition procedures are taken from the mesh points located on the boundary. Mass flow and Mach number boundary condition are used at the highest level grid during the multigrid cycle. The value of resulting pressure is then kept constant through one multigrid cycle on the lower level grids.

V. Test Cases

As test cases, a two-dimensional subsonic channel with constant area and the Royal Airforce Establishment (RAE) M2129 S-duct were calculated. In each case, the benchmarking calculations with the total states inflow boundary condition and the static pressure outflow boundary condition with defined total values p_0 and T_0 and a static value of p were calculated. Mass flow and reference Mach number were then obtained during postprocessing and were used as an input parameter for the tests with mass flow and Mach number boundary conditions. The solutions were then compared. For the RAE M2129 S-duct, testing of the behavior of the mass flow boundary conditions under conditions of choked flow was carried out. In addition, the outflow mass flow boundary condition from Ref. 10 was used, and the results were added to the comparisons. This boundary condition relaxes the value of the static pressure at the outflow boundary to its desired value using

$$p^{k+1} = p^k\left[1 + \Phi\left(\dot{M}_r - \dot{M}^k\right)\big/\dot{M}_r\right] \tag{24}$$

where Φ is a relaxation parameter and $\dot{M}_r$ is the desired mass flow through the outflow boundary. The value of relaxation parameter was chosen as $\Phi = -0.02$.

A. Case 1: Two-Dimensional Subsonic Channel

The subsonic $h = 1$-m-high and $l = 30$-m-long channel has been chosen for the first set of tests. The values used for the benchmark case were the total pressure $p_0 = 101{,}391.22$ Pa, total temperature $T_0 = 300.057$ K at the inflow, and static pressure $p = 101{,}323$ Pa at the outflow. The results of benchmark case are total mass flow through channel $\dot{M} = 10.5187\ \mathrm{kg\cdot s^{-1}}$ and average Mach number at outflow $M = 0.02575$.

Table 1 Total pressure at inflow and static pressure at outflow boundary, subsonic channel case, mass flow boundary conditions (BC)

Case	p_0 at inflow	p at outflow	Final mass flow $\dot{M}$
Benchmark	101,391.22	101,323.00	10.5187
Inflow mass flow BC	101,391.98	——	10.5232
Outflow mass flow BC	——	101,322.32	10.5135
Outflow mass flow BC, Ref. 10	——	101,322.30	10.5187

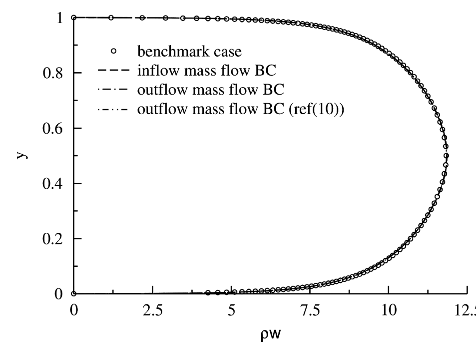

a) Profile of mass flow at $x/h = 27$

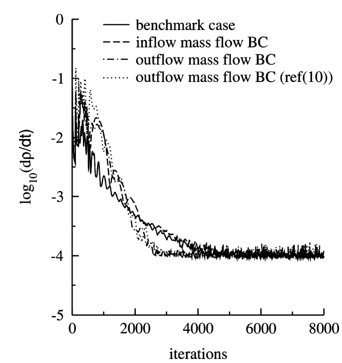

b) Density residuals

Fig. 2 Flow through channel with constant area mass flow boundary conditions (BC).

1. *Two-Dimensional Channel with Mass Flow Boundary Conditions*

Two cases were calculated. In the first case, the total states at inflow and the mass flow boundary condition at outflow were used. In the second case, the mass flow boundary condition was used at inflow and static pressure at outflow. Figure 2a shows the profiles of ρw at position $x/h = 27$ in the channel for both test cases compared to the benchmark case. The results are almost identical for all three types of boundary conditions. The final static pressure for the outflow mass flow boundary condition and total pressure for the inflow mass flow boundary condition were predicted accurately with very low error. These results, together with final values of total mass flow are given in Table 1. A difference occurs in the residuals of the computational process as shown in Fig. 2b. The benchmark case converged well down to a value around $\log_{10}(\mathrm{d}\rho/\mathrm{d}t) \approx -4$. Both outflow mass flow boundary conditions show faster convergence then the benchmark case. The inflow mass flow boundary conditions convergence is almost the same as for the benchmark case.

2. *Two-Dimensional Channel with Outflow Mach Number Boundary Condition*

The outflow Mach number boundary condition was tested in the same flow with prescribed total states at inflow. Final static pressure at the outflow was compared to the value obtained in the benchmark case and is shown in Table 2. The values are almost identical. Mach

Table 2 Predicted static pressures and Mach number at outflow boundary, subsonic channel case, Mach number BC

Case	p at outflow	Final outflow Mach number
Benchmark	101,323.00	0.02575
Outflow Mach number BC	101,323.13	0.02570

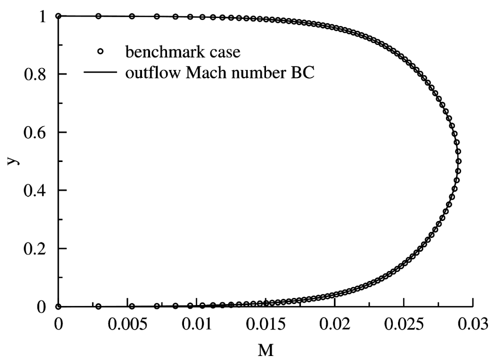

a) Profile of Mach numbers at $x/h = 27$

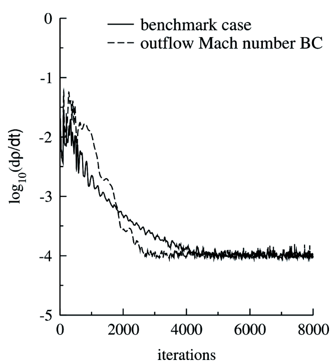

b) Density residuals

Fig. 3 Flow through channel with constant area, outflow Mach number BC.

number profiles at position $x/h = 27$ in the channel are shown in Fig. 3a. The convergence of the computational process with the outflow Mach number boundary condition shown in Fig. 3b is good and is faster than the benchmark case convergence.

B. Case 2: RAE M2129 S-Duct

The second case was the flow through the RAE M2129 S-duct, the geometry of which is defined in Ref. 15. The geometry used for meshing was nondimensionalized by inflow radius. The grid has an extension upstream of the inflow to build an adequate boundary layer on the walls of the S-duct and is also extended downstream of the outflow to avoid flow reversal through the boundary. This S-duct is highly curved so that flow separation occurs at moderate Mach numbers. Large flow separation together with large losses in total pressure makes this case interesting for testing the new set of boundary conditions. The flow structure with vortex liftoff is shown in Fig. 4. It is clear that the zone of large pressure losses does not cover only the boundary layer but extends into the interior of the channel and covers quite a large portion of the S-duct area. As may be expected, setting the mass flow by estimating the total pressure at inflow and static pressure at outflow may lead to a large error in final value of mass flow.

The benchmark case is defined as the one with total state boundary conditions at inflow and static pressure boundary condition at outflow. The values are total pressure $p_0 = 3488.62$ Pa, total temperature $T_0 = 302.85$ K, at inflow, and static pressure $p = 2971.86$ Pa, at outflow. The final value of mass flow calculated from the solution is $\dot{M} = 22.615\,\mathrm{kg\cdot s^{-1}}$ and the average Mach number at outflow is $M = 0.422$.

Table 3 Total pressure at inflow and static pressure at outflow boundary, RAE M2129 S-duct case, mass flow BC

Case	p_0 at inflow	p at outflow	Final mass flow $\dot{M}$
Benchmark	3488.62	2971.86	22.615
Inflow mass flow BC	3487.92	——	22.608
Outflow mass flow BC	——	2969.23	22.619
Outflow mass flow BC, Ref. 10	——	2972.40	22.616

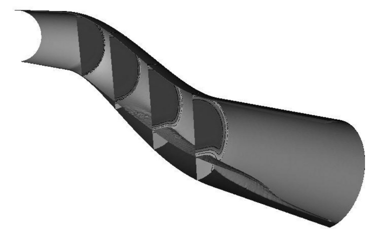

a) Total pressure contours in duct

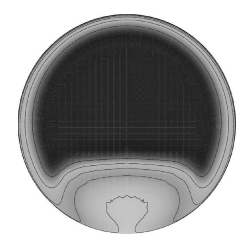

b) Pressure recovery on the engine face

Fig. 4 Flow through RAE M2129 S-duct.

1. RAE M2129 S-Duct with Mass Flow Boundary Conditions

Two cases were calculated. In the first case, the total states were specified at the inflow, and the mass flow was specified at the outflow. In the second case, the mass flow boundary condition was applied at the inflow, and static pressure was specified at outflow. The given value of total mass flow was $\dot{M} = 22.615\,\mathrm{kg\cdot s^{-1}}$. The final values of total pressure at inflow for the inflow mass flow boundary and static pressure at outflow for the outflow mass flow boundary, together with results of the outflow mass flow boundary condition from Ref. 10 are given in Table 3. All values were predicted with rather high accuracy. The maximum mass flow deviation from the benchmark value was only 0.03%. Residuals of the computational process and static pressure at the lower and upper side of the channel are shown in Fig. 5. The convergence of the computational process with the inflow mass flow boundary condition is very similar to the benchmark case convergence. Both outflow mass flow boundary conditions have some effect on the convergence of the computational process; nevertheless, the convergence is good.

The next study included calculations of the RAE M2129 S-duct for several different values of total mass flow. Inflow mass flow boundary conditions were tested for four different mass flow values: $\dot{M} = 16$, 22.615, 25, and 30 $\mathrm{kg\cdot s^{-1}}$ with a constant static pressure at the outflow boundary equal to $p = 2971.86$ Pa. Isolines of Mach number in the symmetry plane of the S-duct, along with residuals of the computational process, are shown in Fig. 6. Table 4 shows the final values of total pressure and values of mass flow for each case. Values of resulting mass flow for subsonic cases match the values of given mass flow with a maximum difference 0.06%. Note in Fig. 6 that the computation with mass flow of $\dot{M} = 30\,\mathrm{kg\cdot s^{-1}}$ is interesting because the flow is choked. In this case, the total mass flow is the same as the critical mass flow, which is determined by the critical throat. The convergence, as well as small oscillations of the final value of total pressure that are of the order of 0.06%, are due to the complicated flow structure, separation behind the terminal shock, and a complicated feedback between the critical throat that determines the maximum value of mass flow through the

Table 4 Predicted total pressures at inflow boundary, RAE M2129 S-duct case, inflow mass flow BC

Given mass flow $\dot{M}$	p_0 at inflow	Final mass flow $\dot{M}$
16	3217.91	15.991
22.615	3487.92	22.608
25	3628.11	24.993
30	4211.03 ± 3.22	29.982 ± 0.018

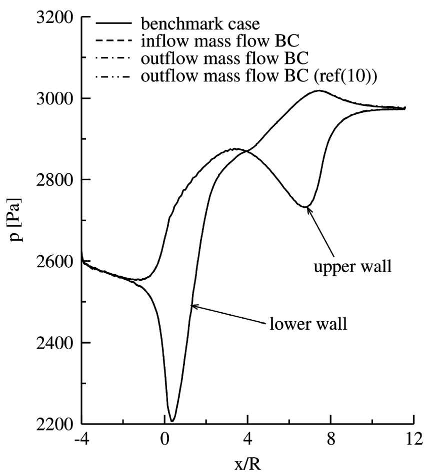

a) Predicted static pressure on lower and upper wall

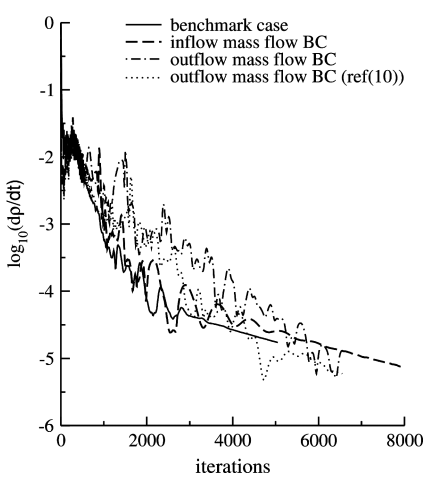

b) Density residuals

Fig. 5 Static pressure and density residuals, RAE M2129 S-duct, inflow and outflow mass flow BC.

Table 5 Predicted static pressures at outflow boundary, RAE M2129 S-duct case, outflow mass flow BC

Given mass flow $\dot{M}$	p at outflow	Final mass flow $\dot{M}$
22.615	2969.23	22.619
24	2854.74	24.011
25	1758.66 ± 9.08	24.993 ± 0.011
28	1536.78 ± 8.72	25.282 ± 0.103
30	1516.57 ± 28.75	25.253 ± 0.394

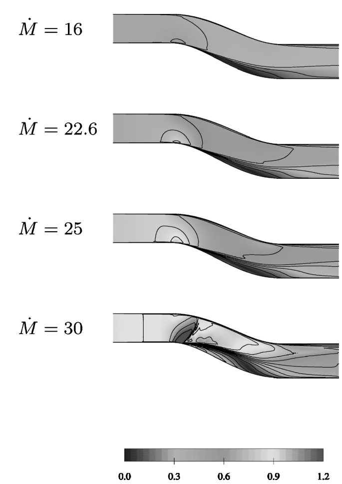

a) Mach numbers

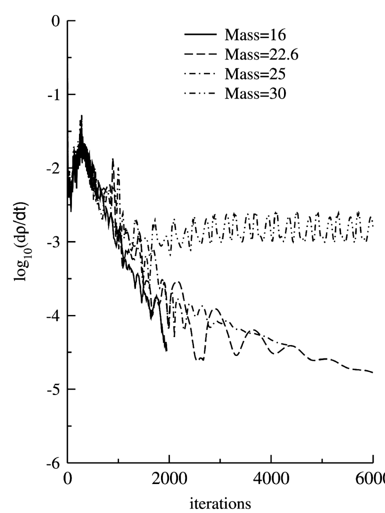

b) Density residuals

Fig. 6 Four different values of total mass flow, RAE M2129 S-duct, inflow mass flow BC.

channel and the inflow mass flow boundary condition that must set an appropriate value of total pressure. Note that the oscillations of mass flow should not be interpreted physically because the flow is solved as steady state.

A similar study with five different prescribed total mass flow values was carried out with outflow mass flow boundary conditions and constant values of total pressure $p_0 = 3488.62$ Pa and total temperature $T_0 = 302.85$ K at inflow. This case is more complicated than the preceding one. As given in Eq. (13), the critical mass flow is dependent on the total values and the area of the critical throat only. Because the total values are fixed, the critical mass flow is to a large extent fixed as well. Figure 7 shows the isolines of the Mach number at the symmetry plane for each case. As might be judged from Fig. 7 as well as from Table 5, the value of the critical mass flow is somewhere around $\dot{M} \approx 25\,\mathrm{kg \cdot s^{-1}}$. For lower values of prescribed mass flow, $\dot{M} = 22.615$ and $24\,\mathrm{kg \cdot s^{-1}}$, the final values of mass flow are the same as the prescribed ones. In the other three cases with higher prescribed values of mass flow, rather complicated choked flows occur with the supersonic area terminated by a terminal shock wave followed by flow separation. The final values of static pressure at outflow as well as the final value of mass flow are oscillatory. As long as the outflow boundary is subsonic as in the case of $\dot{M} = 25\,\mathrm{kg \cdot s^{-1}}$, the amplitude of oscillations is very low. Once part of the boundary becomes supersonic the oscillation of the final value of mass flow becomes substantially larger, which is apparent particularly for the case with a required value of mass flow $\dot{M} = 30\,\mathrm{kg \cdot s^{-1}}$. In these cases, however, the resulting value of static pressure is applied at the subsonic part of the outflow boundary only. Again, because the flowfield is solved as steady state, no physical interpretation of mass flow oscillations can be drawn.

The results of similar study of the choked flow using the outflow mass flow boundary condition from Ref. 10 are shown in Table 6. For values of mass flow up to $\dot{M} = 24\,\mathrm{kg \cdot s^{-1}}$, the results are very similar to their counterparts calculated using a novel outflow mass flow boundary condition. However, when the desired value of mass flow exceeds the critical value of mass flow, which in this case is around $\dot{M} \approx 25\,\mathrm{kg \cdot s^{-1}}$, the solutions are completely different. The

Table 6 Predicted static pressures at outflow boundary, RAE M2129 S-duct case, outflow mass flow BC from Ref. 10

Given mass flow $\dot{M}$	p at outflow	Final mass flow $\dot{M}$
22.615	2972.40	22.616
24	2858.97	23.999
25	2203.61	24.971
28	——	——
30	——	——

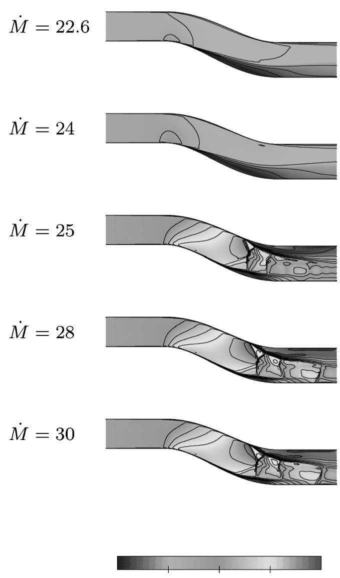

a) Mach numbers

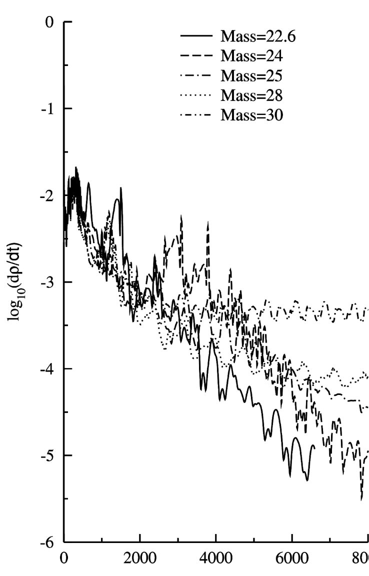

b) Density residuals

Fig. 7 Five different values of total mass flow, RAE M2129 S-duct case, outflow mass flow BC.

explanation of this unexpected behavior may be found in Eq. (24), which is used to update the static pressure on the outflow boundary during the time-marching process. The variable $\dot{M}_{(\mathrm{tot})}$, that represents the actual value of mass flow through the boundary is limited from above by the value of critical mass flow. When the desired value of mass flow $\dot{M}_r$ is larger than the critical value, the term $\dot{M}_r - \dot{M}_{(\mathrm{tot})}$ in Eq. (24) will be larger then zero. Hence, the static pressure will be continually reduced during the time-marching process, ultimately reaching value $p \to 0$. Consequently, there will be a tendency to reduce the amount of mass flow through the boundary. As the value

Table 7 Total pressure at inflow boundary and static pressure at outflow boundary, RAE M2129 S-duct, inflow mass flow and outflow Mach number BC

Case	p_0 at inflow	p at outflow	Final mass flow $\dot{M}$	Final Mach number M
Benchmark	3488.62	2971.86	22.615	0.422
Outflow Mach number BC	——	2972.67	——	0.422
Inflow mass flow and outflow Mach number BC	3488.58	2971.24	22.616	0.422

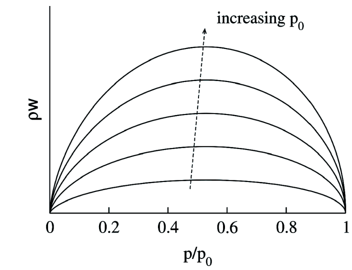

a) Mass flow as function of static pressure

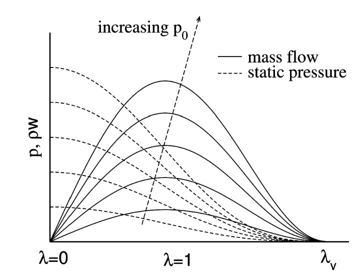

b) Static pressure and mass flow as function of Laval number λ

Fig. 8 Static pressure and mass flow dependencies for different values of total pressure p_0.

of pressure reaches zero, the value of mass flow reaches zero as well, $\dot{M}_{(\mathrm{tot})} \to 0$ (points $p/p_0 = 0$ in Fig. 8a and $\lambda_v = \sqrt{[(\gamma+1)/(\gamma-1)]}$ in Fig. 8b), thus causing singularity at the boundary. From that point of view, as soon as the desired value of mass flow exceeds the critical value, the mass flow boundary condition from Ref. 10 changes the physical character of the flow to a case similar to a shock-tube problem with singularity at the boundary. This represents a problem from both the physical and numerical points of view. The numerical scheme is apparently not able to solve such a difficult case. The solutions for desired values of mass flow $\dot{M} = 28$ and $30\ \mathrm{kg \cdot s^{-1}}$ shown in Fig. 9 are, therefore, identical, mostly low subsonic flows with the discontinuity in front of the outflow boundary and are physically wrong.

Note that when the flow is choked the outflow mass flow boundary condition looses its justification in most cases and should be replaced by another, more suitable boundary condition. The main reason why the choked flow study was carried out was to find out whether the mass flow boundary condition is stable under such difficult conditions and does not diverge, which is important mainly from the user's point of view. However, the ability to handle the choking condition may be useful during the analysis of a supersonic flow in a supersonic inlet. Here, the deceleration of the supersonic flow terminated by a shock wave taking place either in the inlet itself or in the extension of the computational domain behind the inlet, followed by a subsonic flow with an outflow mass flow boundary condition, may represent a reasonable choice for controlling the amount of air flowing through the device.[16,17]

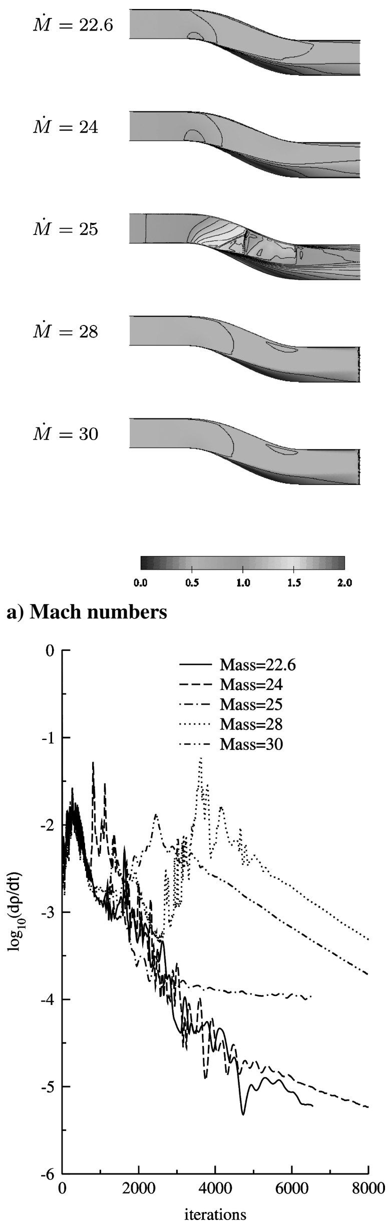

a) Mach numbers

b) Density residuals

Fig. 9 Five different values of total mass flow, RAE M2129 S-duct case, outflow mass flow BC.

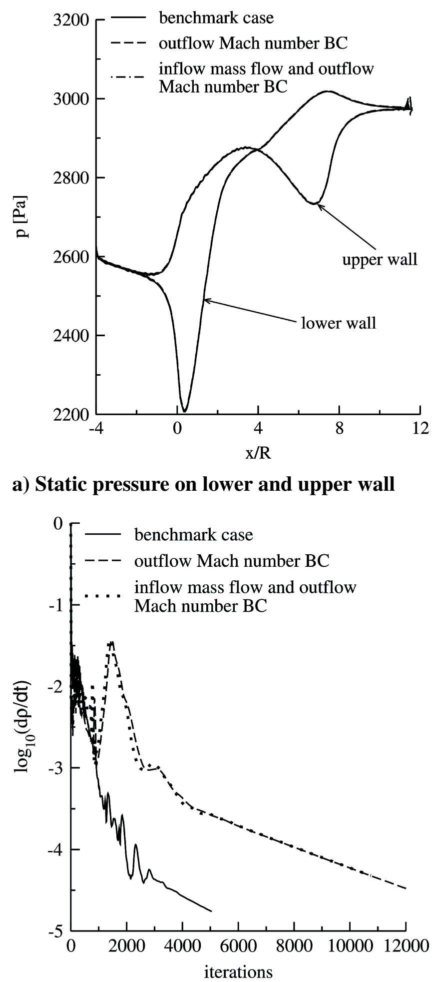

a) Static pressure on lower and upper wall

b) Density residuals

Fig. 10 Static pressure and density residuals, RAE M2129 S-duct, inflow mass flow and outflow Mach number BC.

2. RAE M2129 S-Duct with Mach Number Boundary Condition and with Combination of Mach Number and Mass Flow Boundary Conditions

The next study is the study of flow through an RAE M2129 S-duct with given total states at the inflow and the Mach number outflow boundary condition and also the case with the mass flow boundary condition at inflow and the Mach number boundary condition at outflow. Input values for the mass flow and Mach number boundary conditions were the values of total mass flow $\dot{M} = 22.615\,\mathrm{kg \cdot s^{-1}}$ and a value of averaged outflow Mach number $M = 0.422$. The results are given in Table 7. All values were predicted with good accuracy. Figure 10 shows the static pressure along the upper and lower wall and the residuals of the computational process. The static pressure curves are identical and show that there is no difference between the solutions. The convergence was, however, affected. The slope of convergence curve is very similar to that of the benchmark case; however, the peak in residuals that occurred after approximately 1000 iterations resulted in a higher final value of the residuals. It was concluded that the predominant effect influencing the higher final value of residuals was the Mach number boundary condition.

VI. Conclusions

A new system of boundary conditions enabling direct control of mass flow through a subsonic inflow and outflow boundary was developed and implemented into CFD code. Additionally, the outflow Mach number boundary condition was implemented. The boundary conditions are constructed in such a way that they need only minimal user input and are well posed. The construction of the novel boundary conditions should be rather general, with no strong ties to any specific numerical scheme.

Verification tests were carried out on the flow through a two-dimensional channel with constant area at very low speeds and on the high-speed flow through an RAE M2129 S-duct. Particular attention was paid to testing the behavior of the mass flow boundary conditions in flows that are choked. It was proved that as long as the flow through the boundary is subsonic, the boundary conditions are stable. Once the flow through the boundary becomes supersonic, the final value of mass flow oscillates. Nevertheless, the solution did not diverge and remained stable with higher values of residuals. However, in most of these cases, the mass flow boundary conditions should not be used. All tests carried out were steady-state cases. There were no attempts to calculate the flow for the time-dependent value of the mass flow. None of the test cases required reduction of the Courant–Friedrichs–Lewy number. The numerical scheme was the same for all calculations. The numerical accuracy is not affected by novel boundary conditions.

The relative simplicity of implementation of the new boundary conditions, as well as good stability and efficiency, make the mass flow and Mach number boundary conditions an attractive tool for use in CFD analysis of complex aerodynamic flows.

Acknowledgments

The Swedish Defence Materiel Administration is acknowledged for financing this project. John W. Slater of NASA John H. Glenn Research Center at Lewis Field is acknowledged for useful suggestions and comments on the paper. Jaroslav Pelant of the Aeronautical Research and Test Institute, Czech Republic, is acknowledged for providing details on the results of his outflow mass flow boundary condition. The author is indebted to the editor and anonymous reviewers, whose comments helped to improve the quality of this paper. A special thank you is extended to Stephen Conway and Stefan Jakobsson of the Swedish Defence Research Agency for excellent and patient work during revisions of this paper.

References

[1] Staiger, J. M., "Cobalt$_{60}$ CFD Analysis of the Active Core Exhaust (ACE) System," AIAA Paper 2003-3460, June 2003.

[2] Chuang, H. A., and Verdon, J. M., "A Numerical Simulator for Three-Dimensional Flows Through Vibrating Blade Rows," NASA CR-1998-208511, Aug. 1998.

[3] Zhou, X., and Wolff, M., "Transonic Compressor IGV/Rotor Interaction Analysis Including Fluid Structure Interaction," AIAA Paper 2004-5292, June 2004.

[4] Forsythe, J., Squires, K., Wurzler, K., and Spalart, P., "Prescribed Spin of the F-15E Using Detached-Eddy Simulation," AIAA Paper 2003-839, Jan. 2003.

[5] Morton, S., Steenman, M., Cummings, R., and Forsythe, J., "DES Grid Resolution Issues for Vortical Flows on a Delta Wing and an F-18C," AIAA Paper 2003-1103, Jan. 2003.

[6] Abbott, J. M., and Slater, J. W., "Computational Study of the Aerodynamic Performance of Three-Dimensional Subsonic Inlets," AIAA Paper 2001-3886, July 2001.

[7] Fares, E., Meinke, M., and Schröder, W., "Numerical Simulation of Wingtip Vortices and Engines in the Near Field," AIAA Paper 2000-2222, June 2000.

[8] Conway, S., "Implementation and Validation of an Engine Nacelle Boundary Condition in Edge 3.2," Swedish Defence Research Agency, Technical Rept., FOI-R-1320-SE, Stockholm, 2004.

[9] Berglind, T., and Nordström, J., "Flow Simulation Around a Realistic Fighter-Aircraft Configuration, Including the Influence of the Hot Jet," *Recent Advantages and Applications in Computational Fluid Dynamics*, edited by O. Baysal, AIAA, Washington, DC, 1990, pp. 163–170.

[10] Slater, J. W., "Verification Assessment of Flow Boundary Conditions for CFD Analysis of Supersonic Inlet Flows," AIAA Paper 2001-3882, July 2001.

[11] Pelant, J., and Adámek, K., "Boundary Value Conditions for Some 3D Axis-Symmetrical Flows," European Congress on Computational Methods in Applied Sciences and Engineering, ECCOMAS-CFD Conf., Sept. 2001.

[12] Dvořák, R., *Transonic Flow*, Academia, Academy of Sciences of the Czech Republic Publishing-House, Prague, 1986, pp. 29–33 (in Czech).

[13] Eliasson, P., "EDGE, A Navier–Stokes Solver for Unstructured Grids," *Proc. to Finite Volumes for Complex Applications III*, edited by D. Kroner and R. Herbin, Hermes Penton Science, London, 2002, pp. 527–534.

[14] Wallin, S., and Johansson, A., "A Complete Explicit Algebraic Reynolds Stress Model for Incompressible and Compressible Turbulent Flows," *Journal of Fluid Mechanics*, Vol. 403, 2000, pp. 89–132.

[15] "Air Intakes for High Speed Vehicles," AGARD Advisory Rept. 270, Fluid Dynamics Panel Working Group 13, AR-270, AGARD, Sept. 1991.

[16] Hayes, C., "Preliminary Investigation of a Variable Mass-Flow Supersonic Nose Inlet," NACA RMl9j11, Aug. 1949.

[17] Carrier, G., Knight, D., Rasheed, K., and Montazel, X., "Multi-Criteria Design Optimization of Two-Dimensional Supersonic Inlet," AIAA Paper 2001-1064, Jan. 2001.

C. Bailly
Associate Editor